

Molecular Dynamic Simulations of Forming Graphene Nanoribbons from Single-Wall Carbon Nanotubes

Rongjun Zhang^{1,2} and Hanqing Jiang^{1,*}

¹*School of Mechanical, Aerospace, Chemical, and Materials Engineering, Arizona State University, Tempe, AZ 85287, USA*

²*Department of Physics, Wuhan University, Wuhan, 430072, P. R. China*

Graphene nanoribbons (GNRs) are strips of graphene, a newly discovered material with carbon atoms parked in a two-dimensional honeycomb lattice, has attracted great deal of attention, because of its spectacular properties and various applications. This paper develops a new approach to form GNRs, namely cleaving single-wall carbon nanotubes (SWCNTs) by the bombardment of nanoparticles, by means of molecular dynamics simulations. Nanoparticles are accelerated by an electric field to bombard SWCNTs on substrates. Depending on the offset and relative diameters between nanoparticles and SWCNT, the SWCNTs can be cleaved and unraveled to GNRs. Because of the nanometer-scale of circumference of SWCNTs, the formed GNRs possess nanometer width. The conditions of the molecular dynamics simulations are able to be realized by current experimental capability.

Keywords: Graphene Nanoribbons, Single-Wall Carbon Nanotubes, Molecular Dynamic Simulation.

1. INTRODUCTION

Graphene, a newly discovered material with carbon atoms parked in a two-dimensional honeycomb lattice, has attracted great deal of attention, because of its spectacular properties¹ and various applications,^{2,3} such as sensors,^{4,5} nanocomposites,^{6,7} supercapacitors,^{8,9} and hydrogen storage.^{10,11} Graphene nanoribbons (GNRs), i.e., strips of graphene, gradually transform from semiconductors to semimetals as their width increases,^{12–15} and are predicted to exhibit band gaps useful for room temperature transistor operations with excellent switching speed and high carrier mobility (potentially even ballistic transport) when the ribbon width down to 10 nm.

Various approaches have been developed to synthesize GNRs, including lithographic methods,^{13,16} chemical methods,^{17,18} and physical methods.^{19,20} Lithographic patterning of graphene sheet has fabricated GNRs down to the widths of ~20 nm thus far, but there are difficulties in synthesizing ribbons with width in a few nanometers and smooth edges. The difficulty of scalable production of graphene is also a big obstacle which hampers the further application of lithographic method.²¹ Chemical methods are commonly used to produce various types of nanomaterials and several groups have reported their achievements on the synthesis of GNRs.^{22,23} However, the product yield

of chemical methods was low and the width distribution of GNRs was broad, ranging from less than 10 nm to about 100 nm. As a result, scientific community desires a new approach capable of precisely controlling the synthesis of GNRs.

Geometrically, GNRs and carbon nanotubes (CNTs) share the same honeycomb lattice structure, which makes these two materials more fascinating if they are capable of inter-transforming. Theoretical studies on GNRs,^{24–26} have suggested that GNR edges (especially zigzag edges) have good chemical reactivity due to their unique electronic state near the Fermi level that is localized at the edge carbon atoms. This reactivity leads to the spontaneous emergence (i.e., a self-assembly process) of planar reconstruction for zigzag edges, achievable even at room temperature. Molecular dynamics studies have been conducted to synthesize various CNT junctions (e.g., metal-semiconductor-metal junctions, multi-terminal junctions) from tailored GNR nanoribbons.²⁷

Recently, some researchers have investigated the inverse approach, forming GNRs from CNTs, and some progresses have been achieved. Kosynkin et al.²⁸ utilized a simple solution-based oxidative process for producing a nearly 100% yield of GNR structures by lengthwise cutting and unraveling of multi-walled CNT side walls. This method, however, is difficult to obtain narrow GNRs with band gap efficient for room-temperature transistor applications; moreover, edge oxidation in those small structures may

* Author to whom correspondence should be addressed.

retard their electronic utility. Jiao et al.²⁰ developed controlled unzipping of multi-walled CNTs to produce GNRs by an Ar plasma etching method. It was observed that 20% of the multi-walled CNTs were converted into single- and few-layer GNRs of 10–20 nm width. This approach is also compatible with semiconductor processing, and progress made in the synthesis, size control, placement and alignment control of multi-walled CNTs can be exploited to make GNRs in a controllable fashion.

In this paper, we develop an alternative method to synthesize GNRs from CNTs via molecular dynamic simulations. This method is to utilize accelerated Au nanoparticles to physical bombard the single-walled carbon nanotubes (SWCNTs) in the axial direction of the tube to cleave and unravel the SWCNTs, thus forming GNRs. Section 2 presents the molecular dynamics model. The results and discussions are given in Section 3.

2. MOLECULAR DYNAMICS SIMULATIONS: MODEL AND METHODS

Figure 1 illustrates our model, in which a SWCNT is laid down on a substrate with blue balls representing the carbon atoms that are attached to the substrates. There are various methods to lay CNTs on different type of substrates (hard or soft).²⁹ An Au nanoparticle is placed to bombard the CNT along the axial direction. Different type of nanoparticles have been synthesized experimentally with diameters ranging from 1.5 nm to 2.5 nm made of various materials, such as Au and Ag nanoparticle.^{30–32} The relation between the size of Au nanoparticle and CNT diameter, as well the offset between the Au nanoparticles and CNTs, are to be studied.

The interaction between C–C in CNT is characterized by the Adaptive-Intermolecular Reactive-Empirical-Bond-Order (AIREBO) potential with Lennard-Jones (LJ) potential addition:³³

$$E = \frac{1}{2} \sum_i \sum_{j \neq i} \left[E_{ij}^{\text{REBO}} + E_{ij}^{\text{LJ}} \sum_{k \neq i, j} \sum_{l \neq i, j, k} E_{kijl}^{\text{Torsion}} \right] \quad (1)$$

Here the Reactive-Empirical-Bond-Order (REBO) potential term E_{ij}^{REBO} describes the short-ranged C–C interactions and their reactive capabilities. These interactions have strong coordination-dependence through a bond order parameter, which adjusts the attraction between the i, j



Fig. 1. Model of the molecular dynamic simulations. A single-wall carbon nanotube is placed on a substrate and a nanoparticle collides along the axial direction.

atoms based on the positions of other nearby atoms and thus the multibody dependence is included. The Lennard-Jones potential term E_{ij}^{LJ} contains a series of switching functions so that the short-ranged Lennard-Jones repulsion does not interfere with the energetics captured by the E_{ij}^{REBO} term. It is also different from the standard Lennard-Jones potential by adding longer-ranged interactions. The torsional potential term $E_{kijl}^{\text{Torsion}}$ describes various dihedral angle preferences in hydrocarbon configurations.

The interaction between Au–Au in an Au nanoparticle is characterized by the embedded-atom-method (EAM) potential.³⁴ The total energy of atom i is given by,

$$E_i = F_\alpha \left(\sum_{j \neq i} \rho_\alpha(r_{ij}) \right) + \frac{1}{2} \sum_{j \neq i} \phi_{\alpha\beta}(r_{ij}) \quad (2)$$

Here F_α is the embedding function of the type α atom and is a function of the local electron density ρ_α , which is given by all the background atoms and endows the multibody nature to the EAM potential. Function $\phi_{\alpha\beta}$ is the pair potential between two atoms of type α and β and depends on the interatomic distance r_{ij} . The atom structure of Au nanoparticle is obtained through an annealing NVT (constant temperature ensemble with Nose/Hoover temperature thermostat) relaxation simulation of the bulk gold FCC lattice structure. The potential between C–Au is characterized by a Lennard-Jones potential.³⁵

Molecular dynamic simulator LAMMPS is used in this study. The model system consists a SWCNT with length about 16 nm and diameter around 1.5 nm laying on a substrate, and several Au nanoparticles carrying one elementary charge, as shown in Figure 1. The Au nanoparticles are placed to offset the center of the SWCNT. Electrical field drives the Au nanoparticles to bombard the SWCNT along the axial direction.

The system is subjected to non-periodic and fixed boundary condition, and all the simulations of bombardment are conducted in a constant energy ensemble NVE. A temperature rescaling is implemented as the thermostat. The velocity-Verlet algorithm is used in the simulation and the time step is set to 0.5 fs. The atoms that contact with the substrate, i.e., the blues ones in Figure 1, are fixed in the simulation. An energy minimization scheme is applied to the initial system and a run up to 100000 steps (i.e., 50 ps) is carried out.

3. RESULTS AND DISCUSSION

We first simulate the bombardment of a (12, 10) chiral CNT with diameter of 1.5 nm by Au nanoparticles with 2.0 nm in diameter. The offset, defined by the center-to-center distance between the Au nanoparticle and CNT, is 0.3 nm. The system has 3161 atoms (2912 C atoms and 249 Au atoms), and the incident kinetic energy of Au nanoparticle is set to be 5000 eV. The process of bombardment is shown in Figure 2. After the bombardment

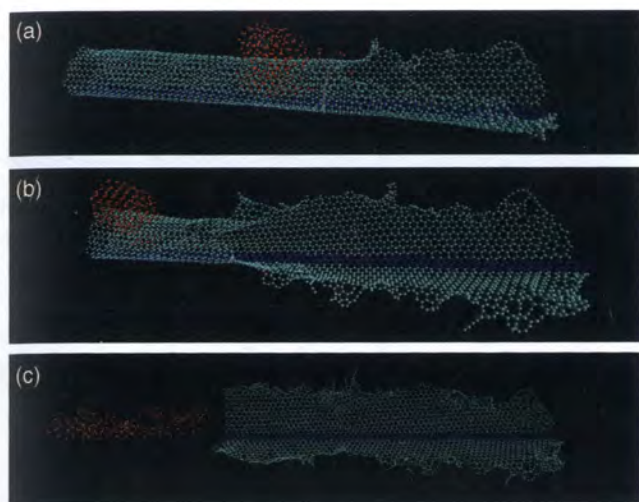


Fig. 2. Cleaving a (12, 10) single-wall carbon nanotube (SWCNT) by the bombardment of three Au nanoparticles. (a), (b): First and second Au nanoparticles partially unravel the SWCNT and (c) the third Au nanoparticle completes unravel the SWCNT.

of the first Au nanoparticle (Fig. 2(a)), the forefront of the SWCNT is cleaved and unraveled, thus forming one section of graphene with irregular edges. Meanwhile, the Au nanoparticle is also cleaved to two parts that both move along the axial direction of CNT and few Au atoms stay in or around the CNT. Then the second Au nanoparticle is accelerated and bombarded the partially unraveled CNT (Fig. 2(b)). This process further cleaves the CNT. After the bombardment from the third Au nanoparticle, the entire CNT is cleaved and a GNR with length 16 nm and width about 4.5 nm is formed. The edge of this formed GNR is irregular, which is mainly resulted from the high velocity of the nanoparticles. This edge defects are possibly smoothed out by a further Joule heating process.³⁶

The cleavage of CNT by Au nanoparticles' bombardment depends on the offset and the diameter of Au nanoparticles. Intuitively, the influence of these two effects can be categorized into three cases as illustrated in Figure 3. First, we discuss the case in which the diameter of the Au nanoparticles is slightly greater than that of the SWCNTs. When the offset is smaller than the radius of the SWCNT (Fig. 3(a)), the Au nanoparticles may cleave the SWCNT. When the offset is the same or slightly greater than the radius of the SWCNT (Fig. 3(b)), normal collision may occur and the Au nanoparticles may be reflected back, which may not cleave the SWCNT. When the offset is greater than the radius of the SWCNT (Fig. 3(c)), the Au nanoparticle may slip away and the SWCNT may not be cleaved. Next, we discuss the case in which the diameter of the Au nanoparticles is less than that of the SWCNTs. When the offset is smaller than the radius of the SWCNT (Fig. 3(d)), the Au nanoparticles may pass through and the SWCNT remains intact. When the offset is the same or greater than the radius of the SWCNT, the Au nanoparticles may be reflected back (similar to Fig. 3(b)) or

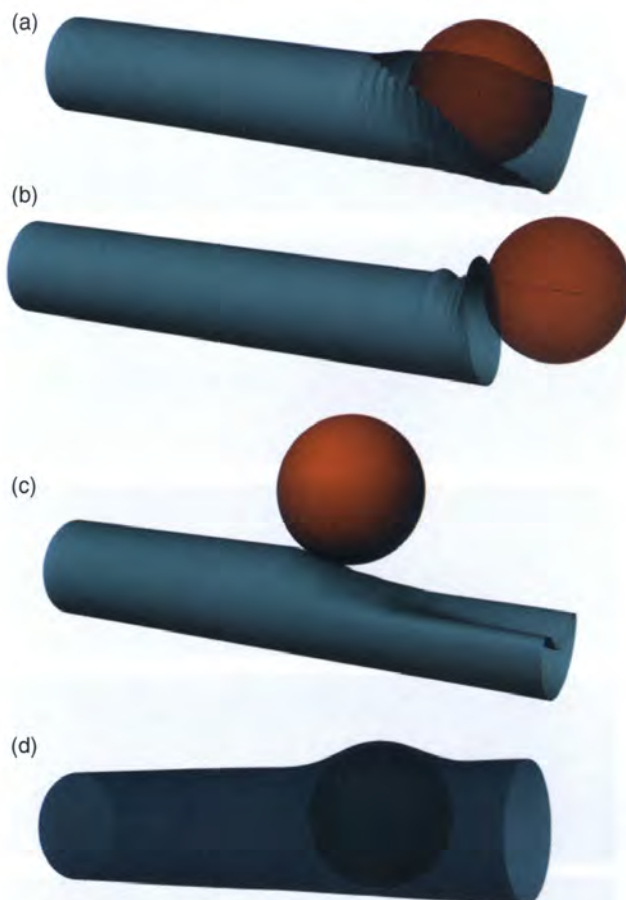


Fig. 3. Illustrations showing the offset and diameter effects.

slip away (similar to Fig. 3(c)), which may not cleave the SWCNT. For Au nanoparticles with diameter much greater than the diameter of the SWCNT, no matter the offset, the Au nanoparticles cannot cleave the SWCNT and have to either be reflected back (similar to Fig. 3(b)) or slip away (similar to Fig. 3(c)).

To study the offset effect, the diameter of Au nanoparticles is kept as 2 nm, larger than the diameter of the (12, 10) SWCNT 1.5 nm. Different offsets are chosen. Offsets for Figures 4(a–c) are 0.4 nm, 0.6 nm, and 0.7 nm, respectively, which corresponds to the case that the offset is less than the radius of SWCNT (Fig. 3(a)). It shows that the SWCNTs are cleaved by the Au nanoparticles. When the offsets are the same or slightly greater than the radius of the SWCNT (Fig. 3(b)), specifically, 0.75 nm and 0.9 nm for Figures 4(d) and (e), respectively, the normal collisions occur and the SWCNTs are not cleaved by the Au nanoparticles. When the offset is 1.05 nm (Fig. 4(f)), Au nanoparticles slip away, consistent with the picture given by Figure 3(c).

The effect of the Au nanoparticles diameters is then studied. Figures 2 and 4 have shown the bombardment behavior of Au nanoparticles with diameters slightly larger than the diameter of the SWCNT. Figure 5(a) shows that an Au nanoparticle with diameter of 2.3 nm, much larger than the diameter of SWCNT, is reflected back, which

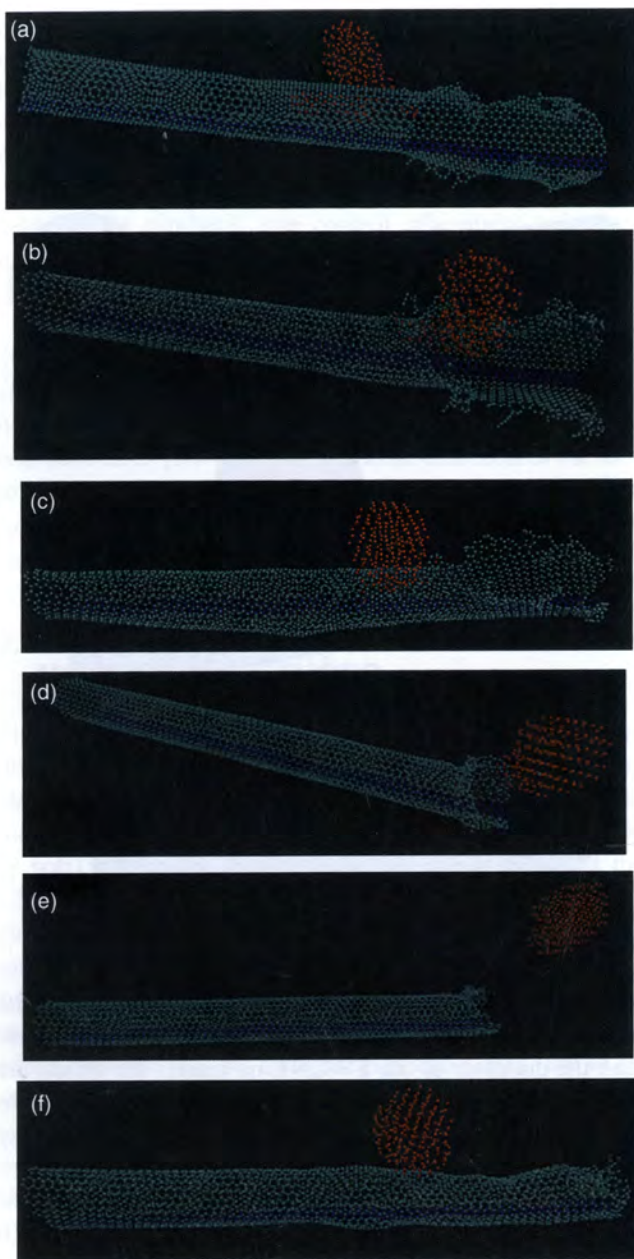


Fig. 4. Molecular dynamic simulation results show the offset effects.

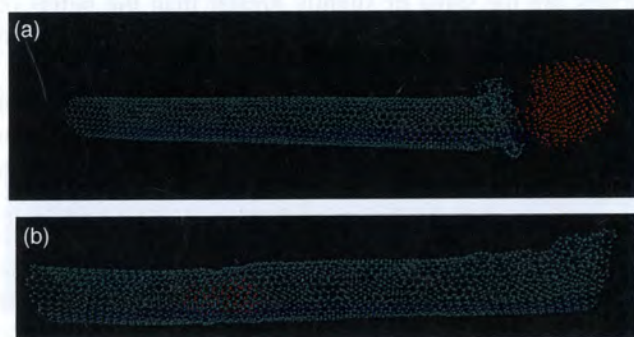


Fig. 5. Molecular dynamic simulation results show the effect of diameter of nanoparticles.

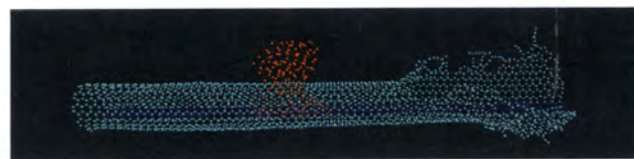


Fig. 6. Molecular dynamic simulations show that this bombardment method can also unravel armchair single wall carbon nanotube (SWNT). Here a (10, 10) armchair SWNT is unraveled by an Au nanoparticle.

agrees with the case given by Figure 3(b). For an Au nanoparticle with diameter of 1.6 nm and offset 0.3 nm (Fig. 5(b)), the nanoparticle passes through without cleaving the SWCNT, consistent with Figure 3(d).

The aforementioned simulations are for (12, 10) chiral SWCNTs. The cleavage behavior of SWCNT by the bombardment of nanoparticles is also observed for other SWCNT. For example, Figure 6 shows that a (10, 10) armchair with diameter of 1.4 nm and length of 16 nm can be cleaved by a Au nanoparticle with diameter of 1.9 nm.

4. CONCLUSION

This paper develops an alternative approach to form GNRs, namely cleaving SWCNTs by the bombardment of nanoparticles, by means of molecular dynamics simulations. Nanoparticles are accelerated by an electric field to bombard SWCNTs on substrates. Depending on the offset and relative diameters between nanoparticles and SWCNT, the SWCNTs can be cleaved and unraveled to GNRs. Because of the nanometer-scale of circumference of SWCNTs, the formed GNRs possess nanometer width. The conditions of the molecular dynamics simulations are able to be realized by current experimental capability. This work is complementary to the inverse process of forming CNTs from GNRs. The interplay of these two processes is able to establish more intimate bridge between CNTs and GNRs with versatile applications.

Acknowledgment: The authors acknowledge the High Performance Computing Initiative (HPCI) at the Arizona State University. Rongjun Zhang acknowledges the financial support from the China Scholarship Council.

References

1. A. H. Castro Neto, F. Guinea, N. M. R. Peres, K. S. Novoselov, and A. K. Geim, *Reviews of Modern Physics* 81, 109 (2009).
2. A. K. Geim and K. S. Novoselov, *Nat. Mater.* 6, 183 (2007).
3. M. I. Katsnelson, *Mater. Today* 10, 20 (2007).
4. J. D. Fowler, M. J. Allen, V. C. Tung, Y. Yang, R. B. Kaner, and B. H. Weiller, *ACS Nano* 3, 301 (2009).
5. F. Schedin, A. K. Geim, S. V. Morozov, E. W. Hill, P. Blake, M. I. Katsnelson, and K. S. Novoselov, *Nat. Mater.* 6, 652 (2007).
6. S. Stankovich, D. A. Dikin, G. H. B. Dommett, K. M. Kohlhaas, E. J. Zimney, E. A. Stach, R. D. Piner, S. T. Nguyen, and R. S. Ruoff, *Nature* 442, 282 (2006).

7. T. Ramanathan, A. A. Abdala, S. Stankovich, D. A. Dikin, M. Herrera-Alonso, R. D. Piner, D. H. Adamson, H. C. Schniepp, X. Chen, R. S. Ruoff, S. T. Nguyen, I. A. Aksay, R. K. Prud'Homme, and L. C. Brinson, *Nat. Nano* 3, 327 (2008).
8. S. Vivekchand, C. Rout, K. Subrahmanyam, A. Govindaraj, and C. Rao, *J. Chem. Sci.* 120, 9 (2008).
9. M. D. Stoller, S. Park, Y. Zhu, J. An, and R. S. Ruoff, *Nano Lett.* 8, 3498 (2008).
10. G. K. Dimitrakakis, E. Tylianakis, and G. E. Froudakis, *Nano Lett.* 8, 3166 (2008).
11. J. O. Sofo, A. S. Chaudhari, and G. D. Barber, *Phys. Rev. B* 75, 153401 (2007).
12. D. A. Areshkin, D. Gunlycke, and C. T. White, *Nano Lett.* 7, 204 (2006).
13. M. Y. Han, B. Ozyilmaz, Y. Zhang, and P. Kim, *Phys. Rev. Lett.* 98, 206805 (2007).
14. K. Nakada, M. Fujita, G. Dresselhaus, and M. S. Dresselhaus, *Phys. Rev. B* 54, 17954 (1996).
15. Y.-W. Son, M. L. Cohen, and S. G. Louie, *Phys. Rev. Lett.* 97, 216803 (2006).
16. Z. Chen, Y.-M. Lin, M. J. Rooks, and P. Avouris, *Physica E: Low-Dimensional Systems and Nanostructures* 40, 228 (2007).
17. A. Yu, P. Ramesh, M. E. Itkis, E. Bekyarova, and R. C. Haddon, *J. Phys. Chem. C* 111, 7565 (2007).
18. E. Rollings, G. H. Gweon, S. Y. Zhou, B. S. Mun, J. L. McChesney, B. S. Hussain, A. V. Fedorov, P. N. First, W. A. de Heer, and A. Lanzara, *J. Phys. Chem. Solids* 67, 2172 (2006).
19. X. Yang, X. Dou, A. Rouhanipour, L. Zhi, H. J. Rader, and K. Mullen, *J. Am. Chem. Soc.* 130, 4216 (2008).
20. L. Jiao, L. Zhang, X. Wang, G. Diankov, and H. Dai, *Nature* 458, 877 (2009).
21. R. Sharma, N. Nair, and M. S. Strano, *J. Phys. Chem. C* 113, 14771 (2009).
22. X. Li, X. Wang, L. Zhang, S. Lee, and H. Dai, 319, 1229 (2008).
23. J. Campos-Delgado, J. M. Romo-Herrera, X. Jia, D. A. Cullen, H. Muramatsu, Y. A. Kim, T. Hayashi, Z. Ren, D. J. Smith, Y. Okuno, T. Ohba, H. Kanoh, K. Kaneko, M. Endo, H. Terrones, M. S. Dresselhaus, and M. Terrones, *Nano Lett.* 8, 2773 (2008).
24. P. Koskinen, S. Malola, and H. Hakkinen, *Phys. Rev. Lett.* 101, 115502 (2008).
25. D. E. Jiang, B. G. Sumpter, and S. Dai, *J. Chem. Phys.* 126, 134701 (2007).
26. A. J. Du, S. C. Smith, and G. Q. Lu, *Nano Lett.* 7, 3349 (2007).
27. H. Lan, L. Jun-Qiang, and J. Hanqing, 5, 2802 (2009).
28. D. V. Kosynkin, A. L. Higginbotham, A. Sinitskii, J. R. Lomeda, A. Dimiev, B. K. Price, and J. M. Tour, *Nature* 458, 872 (2009).
29. D. Y. Khang, J. L. Xiao, C. Kocabas, S. MacLaren, T. Banks, H. Q. Jiang, Y. Y. G. Huang, and J. A. Rogers, *Nano Lett.* 8, 124 (2008).
30. K. Dick, T. Dhanasekaran, Z. Zhang, and D. Meisel, *J. Am. Chem. Soc.* 124, 2312 (2002).
31. A. Henglein, *Langmuir* 15, 6738 (1999).
32. W. Li, Q. X. Jia, and H.-L. Wang, *Polymer* 47, 23 (2006).
33. B. Ni, S. B. Sinnott, P. T. Mikulski, and J. A. Harrison, *Phys. Rev. Lett.* 88, 205505 (2002).
34. L. J. Lewis, P. Jensen, and J.-L. Barrat, *Phys. Rev. B* 56, 2248 (1997).
35. S. Arcidiacono, J. H. Walther, D. Poulikakos, D. Passerone, and P. Koumoutsakos, *Phys. Rev. Lett.* 94, 105502 (2005).
36. X. Jia, M. Hofmann, V. Meunier, B. G. Sumpter, J. Campos-Delgado, J. M. Romo-Herrera, H. Son, Y. P. Hsieh, A. Reina, J. Kong, M. Terrones, and M. S. Dresselhaus, *Science* 323, 1701 (2009).

Received: 2 June 2010. Accepted: 7 June 2010.